Effect of Vibrational Strong Coupling on controlling the vibrational ladder of excited state

KRIPA MERIN JOSEPH

MS14133

A dissertation submitted for the partial fulfillment of

BS-MS dual degree in Chemical Science

Indian Institute of Science Education and Research Mohali

April 2019

CERTIFICATE

This is to certify that the dissertation titled "**Effect of Vibrational Strong Coupling controlling the vibrational ladder of excited state**" submitted by Ms. Kripa Merin Joseph (Reg.No.MS14133) for the partial fulfillment of BS-MS dual degree programme of the Institute, has been examined by the thesis committee duly appointed by the Institute. The committee finds the work done by the candidate satisfactory and recommends that the report be accepted.

Dr Arjit Kumar De	**Dr. P. Balanarayan**	**Dr. Jino George**
Assistant Professor	Assistant Professor	Assistant Professor (Supervisor)

Dated: April xx, 2019

DECLARATION

The work presented in this dissertation has been carried out by me under the guidance of **Dr. Jino George** at the Indian Institute of Science Education and Research Mohali.

This work has not been submitted in part or in full for a degree, a diploma, or a fellowship to any other university or institute. Whenever contributions of others are involved, every effort is made to indicate this clearly, with due acknowledgment of collaborative research and discussions. This thesis is a bonafide record of original work done by me and all sources listed within have been detailed in the bibliography.

Kripa Merin Joseph
(MS14133)
Dated: April xx, 2019

In my capacity as the supervisor of the candidate's project work, I certify that the above statements by the candidate are true to the best of my knowledge.

Dr. Jino George
(Supervisor)

Acknowledgment

I would like to express the deepest appreciation to my thesis guide **Dr. Jino George** for his consistent guidance and advice during the entire project. Without his guidance and persistent help, this dissertation would not have been possible.

I would like to thank my committee members, Dr. P Balanarayan and Dr. Arijit K De whose valuable suggestions and constructive comments helped me to accomplish this project.

I am grateful to all the lab members for the constructive discussions that we had over tea sessions. I would like to express my special gratitude to Ms. Jyoti and Ms. Pooja for positive suggestions and motivation throughout the project. I am also thankful to Akhila, Jaibir and Yogendra for their consistent support.

I would also like to thank IISER Mohali and DCS facility for instrumental and infrastructural facilities without which this project would not have been completed.

I would also like to express my heartfelt gratitude to my parents for their constant love and support.

Special thanks to Alkins for keeping up research enthusiasm and positive vibe throughout the project.

List of tables

List of figures

ABBREVIATIONS

BOA	benzoylacetone
CyHxO	cyclohexanone
VSC	Vibrational Strong Coupling
USC	Ultra Strong Coupling
CCl_4	Tetrachloride
DBM	dibenzoylmethane
FPC	Fabry Perot Cavity
TDM	Transition dipole moment
CPO	Cyclopentanone

CONTENT

ABSTRACT

When a molecular transition and a resonant optical cavity mode strongly interact by photon exchange, new hybrid light-matter states called as polaritonic states are generated. Generation of polaritonic states modifies the physical and chemical properties of the coupled system. It has already been shown that strong coupling affects the ground state electronic configuration as well as its vibrational envelope. In the current project, we studied the effect of vibrational strong coupling (VSC) on controlling the vibrational ladder in the electronic excited state. Benzoylacetone and coumarin are chosen as model systems for present study. Cooperative VSC effect was incorporated by selective overlapping of solvent vibrational frequency with the carbonyl stretching modes of benzoylacetone and coumarin molecules. Here, we have shown that VSC can affect the vibrational ladder of an excited electronic state through cooperative interactions. The fundamental change in the vibrational frequency and also the reshuffling of the vibrational wavefunction in the excited state modify the F-C transition and hence could affect the transition dipole moment of the system. Cavity tuning experiments clearly shows fluctuation behavior in the electronic absorption spectrum, thus proving the existence of vacuum field.

CHAPTER I

1. INTRODUCTION

Cavity quantum electrodynamics is related to the study of simplest light-matter interaction: two level emitter and a photonic mode. In the beginning, it was associated with quantum optics, where an atom or atomic ensemble is confined in the electromagnetic field in high finesse cavity.[1] Depending upon the ratio of coupling strength per photon and irreversible losses for both emitter and photonic mode, the regime could be classified into weak, strong and ultra strong coupling. In weak coupling regime, losses dominate and lifetime gets modified because of the confinement in cavity whereas in strong coupling regime, coupling dominates that leads to the formation of two new eigen states of system-polaritonic states. In ultra strong coupling regime, the splitting ratio is larger than 10%. [47] In this chapter we will briefly introduce the concept of light-matter interaction and then describe the theoretical framework.

1.1 HISTORICAL BACKGROUND

System is said to be in strong coupling regime when two oscillators strongly couple such that they develop two normal modes and display anti crossing dispersive behavior. Strong coupling regime was experimentally investigated for the first time in 1975 by coupling thin film local oscillator vibrations which were later theoretically proved.[2] In 1983, self-induced Rabi oscillations were reported by Haroche et al. in two-level sodium Rydberg atoms inside an F-P cavity.[3] Nine years later, strong coupling between semiconductor excitons (electron-hole pairs) and F-P cavity in GaAs quantum wells was experimentally shown by Weisbuch and others.[4] After several decades, interaction between single two-level solid state system and single photon on a superconducting chip was demonstrated by Wallraff et al. Rabi splitting of 300meV was observed when cyanine J aggregates were placed within a metallic microcavity. [48] In 2011, it was demonstrated that photochromic materials could enable reversible switching from strong to weak coupling regime.[5] Rabi splitting of 700meV was achieved by coupling electronic

transition using photochromic material combined with both plasmonic structure and F-P cavity.[6] Later in the year 2012, Hutchison et al. demonstrated that chemical reaction can be influenced by strongly coupling vacuum fields to excited electronic landscapes involved in molecular isomerization.[7] Two years later, same group showed that strong coupling is not just limited to electronic transition.[8,10] Ground state molecular vibrations were strongly coupled with the vacuum field of cavity leading to the formation of vibro – polaritonic states. Studies of Raman scattering showed that collective Rabi splitting occurs at the level of a single selected bond.[9] For the first time, strong coupling of ground state molecular vibrations was investigated in solid state and later in liquid phase. Sparks et al. coupled C≡N bond in organometallic complex in liquid phase.[10] Anoop et al. reported significant result which confirmed that rate of reaction can be decreased by vibrational strong coupling.[11] Thus confirming that potential energy surfaces get modified due to VSC. On the other hand under different conditions, it was showed by Hiura et al that rate of a reaction can be accelerated under vibrational strong coupling.[12] Ground state reactivity landscape can also be tilted using vibrational strong coupling.[18] VSC can thus provide new pathway to obtain regioselectivity that cannot be obtained via synthetic routes.[13]

1.2 THEORETICAL PERSPECTIVE

1.2.1 STRONG COUPLING REGIME

In strong coupling regime, exchange energy is faster than any other relaxation process. When molecular transition and a resonant optical cavity mode enter into strong coupling regime, two new hybrid states are generated, both having features of light and matter called polaritonic states. In weak coupling regime, Rabi splitting is lower than original transition energy, where radiative properties get modified. For example in Purcell effect, radiative rate constant and emission quantum yield of excited state gets modified. [14,47]

Wavefunctions of polaritonic states generated via Hopfield – Bogoliubov method:

$$| P+ > = c_{11}|e >_m|0>_c + c_{12}|g>_m|1>_c$$

$$| P- > = c_{22}|e >_m|0>_c + c_{21}|g>_m|1>_c$$

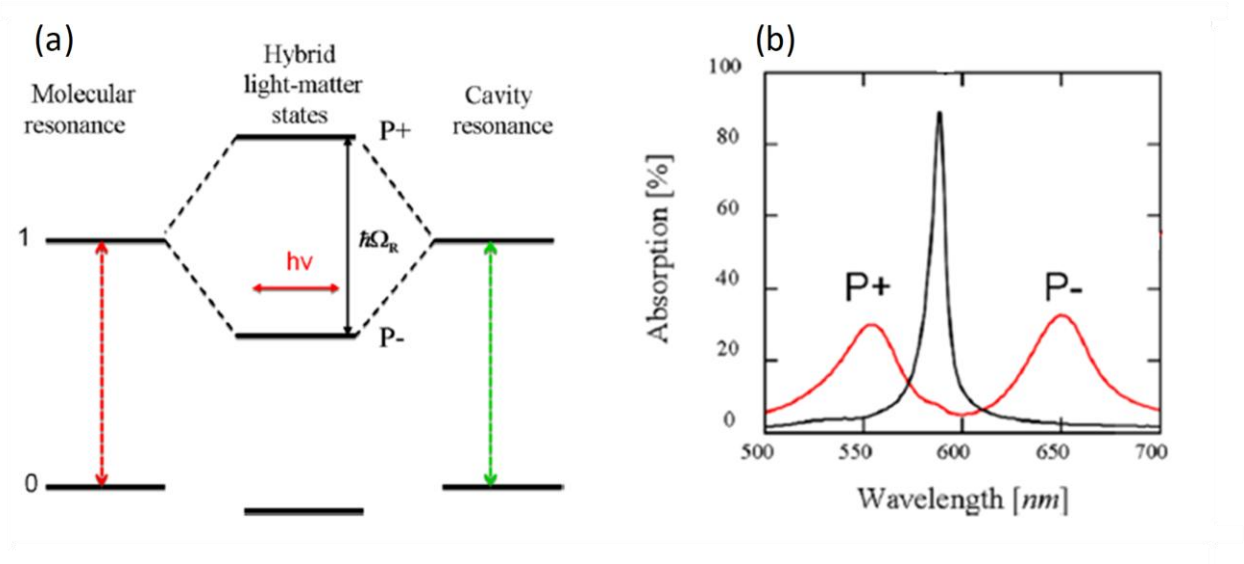

Figure 1.1. (a) Two-level atom and resonant cavity photon mode enters strong coupling regime leading to the formation of two new hybrid states |P+> and |P->. (b) Black spectrum represents the transmission of empty cavity mode, and red one depicts the double-peaked transmission spectrum due to the formation of two new eigenstates. Figure is taken from Ref 15.

The process of formation of | P+ > and | P- > is known as light – matter strong coupling as shown in Figure 1.1(a), | P+ > and | P- > are the combination of Fermionic electronic and Bosonic photonic part. | P+ > and | P-> are separated by Rabi splitting

$$\hbar\Omega_R \quad \alpha \quad \sqrt{\frac{N}{V}}$$

where N is the number of molecules coupled to the optical cavity.

All the molecules are not coupled at the same time as molecules oriented randomly results in averaging out of the interaction and splitting energy can be accounted for those molecular transitions which are parallel to the electromagnetic field of cavity. Rabi splitting can be obtained by coupling molecular ensembles in simple F-P cavities. F-P cavities are plane parallel

mirrors consisting of two opposing flat mirrors. In Figure 1.2(a), F-P cavity shown has two mirrors M1 and M2, with reflectance R1 and R2 separated by a medium of refractive index n and length L. Free Spectral Range (FSR) or frequency difference between two consecutive modes m and m+1 .[16]

$$v_f = \frac{c}{2nL}$$

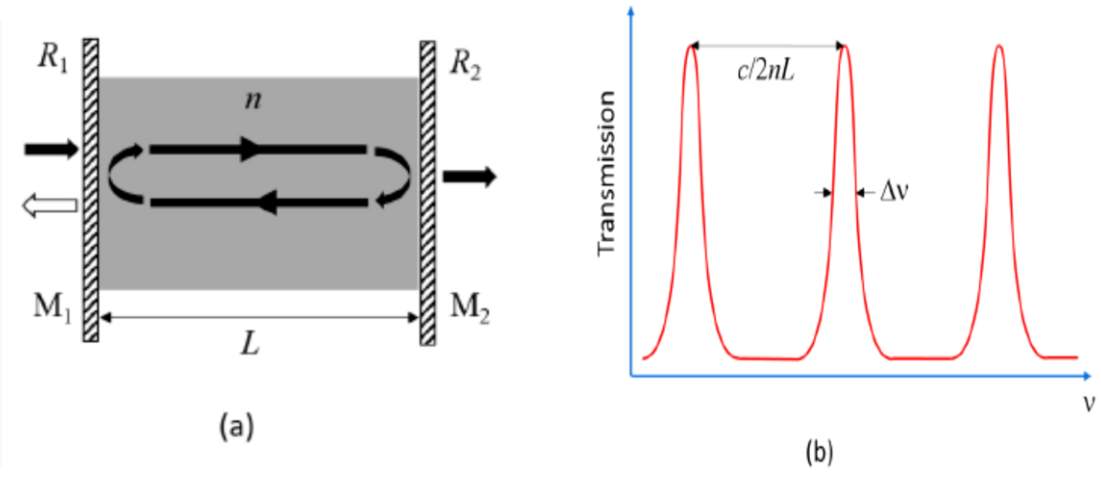

Figure 1. 2(**a**) Schematic of an F-P resonator consisting of parallel mirrors M1 and M2 with reflectances of R1 and R2, respectively, surrounding a cavity medium of refractive index n and thickness L. Light introduced from one side undergoes multiple reflections, leading to partial transmission from the other side;(**b**) Transmission of a planar F-P cavity depicting equi-spaced cavity modes with vf as the FSR, can be calculated from the difference in frequency between adjacent modes measured at peak maximum. The full-width at half-maximum(FWHM) is represented as ΔV. Figure taken from Ref [16].

Rabi splitting can explained by considering Jaynes- Cumming two state model,

$$\Delta E = E_+ - E_- = \hbar\Omega_R = \sqrt{4V_n - (\gamma_c - \gamma_e)^2}$$

Where γ_c and γ_e are decay constants ($\gamma = \hbar/\tau$) of cavity and excited state, E_+ and E_- are energies of |P+ > and |P- >, $V_n = d.E_0$; is the energy between electromagnetic field of cavity and dipole moment of the molecule. In the absence of dissipation, Rabi splitting gets modified to :

$$\hbar\Omega_R = 2V_n = 2d.E_0 = \sqrt{\frac{\hbar\omega}{2\varepsilon_0 \nu}} X \sqrt{n_{photons} + 1}$$

where ħω is the resonant energy, ε_0 is the vacuum permittivity, $n_{photons}$ is the number of photons involved in coupling and ν is the volume of electromagnetic mode.

Above equation shows that splitting can occur even in the absence of photons,when $n_{photons} = 0$, due to interaction between molecular transition dipole and zero point energy fluctuations of cavity mode. Zero point energy of cavity interacts with molecular transition due to exchange of virtual photons.[23] This residual splitting is known as vacuum Rabi splitting. Vacuum fluctuations was reported primarily in Planck's blackbody radiation in 1911 and later in 1913 by Einstein to explain molecular agitation at zero temperature.[21][22]

Light matter hybridization is expected to alter the properties of the system. It has already been shown that coupling of electronic transition and plasmonic mode or cavity mode modifies properties such as conductivity,[24] work function of organic molecule,[25] photochemical isomerization reaction rate,[7] chemical landscape related to reactivity,[7] transport properties, superradiance,[27] coupled electronuclear dynamics and so on. Light matter strong coupling is not limited to electronic transition. Ground state molecular vibrational modes can be hybridized via strong coupling with optical mode of cavity in the infrared region leading to the generation of two new coherent states known as vibro – polaritonic states as shown in Figure 1.3. VSC alters the vibrational energy of molecules thus altering the physical and chemical properties of the molecular ensemble. Since two new coherent states or two new vibrational modes are formed, it strengthens/softens the bond as

$\omega \alpha \sqrt{\frac{f}{\mu}}$, Where f is the bond strength and μ is the reduced mass, assuming that μ does not change under VSC.

Since the change in the vibrational band modifies the Morse potential co-ordinate, the chemical and physical properties of the coupled system get modified.

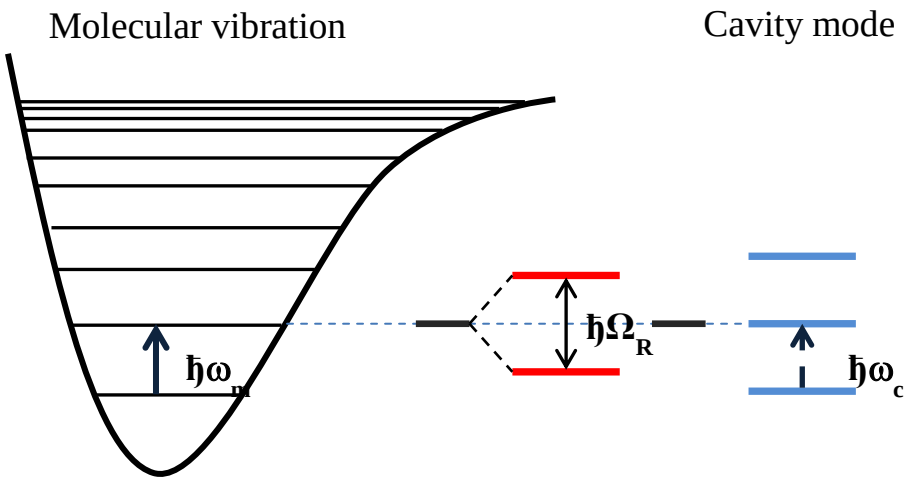

Figure 1.3 Vibrational strong coupling

1.2.2 LIGHT MATTER COUPLING WITH N MOLECULES

Many approximations are required to theoretically explain the model. First one being dipole approximation or long wavelength limit which supposes that wavelength of electromagnetic field is larger than the length of the molecule. This implies that coupling happens only between transition dipole moment of molecule and electric field. Thomson Lorentz model of atom is the second approximation applied here which states that atomic ensemble is the accumulation of oscillators. Before going to the theoretical models for describing light matter strong coupling, transition dipole moment needs to be considered here. Transition dipole moment determines how strongly the system interacts with the electromagnetic wave, i.e, how intense transition would be.

$$\vec{\tau} = < \Psi_f | \vec{\tau} | \Psi_i > = \int \Psi_f | \vec{\tau} | \Psi_i d\tau$$

Therefore, dipolar coupling, here, coupling between light and matter,

$$V = -\vec{\tau}.\vec{\varepsilon}$$

Some of the theoretical models that were used to study organic molecules coupled to light are Jaynes-Cummings (J-C) model (described above) and Tavis-Cummings (T-C) model (or Dicke's models). In Jaynes-Cummings model, a two level emitter and photon gets strongly coupled to generate lower and upper polaritons.

$$\hat{H}_{JC} = \omega_c \hat{a}^\dagger \hat{a} + \omega_s \sigma^+ \sigma^- - g_s(a^\dagger \sigma_- + a\sigma^+)$$

In Tavis-Cummings model single mode of electromagnetic field get coupled to a collection of N molecules under rotating wave approximations. That is, N emitters interact strongly with a photon to yield lower and upper polaritons and N-1 dark states where dark states do not couple with light and thus maintain emitter energy.[20] In other way, when N identical emitters interact strongly with cavity photon, Jaynes-Cumming model becomes Tavis-Cummings model. Both models are shown in Figure 1.4.

$$\hat{H}_{TC} = \omega_c \hat{a}^\dagger \hat{a} + \omega_s \sum_{i=1}^{N} \sigma_i^+ \sigma_i^- - g_s \sum_{i=1}^{N} (a^\dagger \sigma_i^- + a\sigma_i^+)$$

In the year 2018, Jonathan Kelling introduced Holstein Tavis Cumming model (H-T-C model) to bring in coupling between molecular conformation and electronic states which leads to vibrational bands in absorption and emission spectra. Such a model can explain the interaction between the vibrational ladder in electronic state and resonant optical cavity mode.[29] HTC model is schematically shown in Figure 1.5.

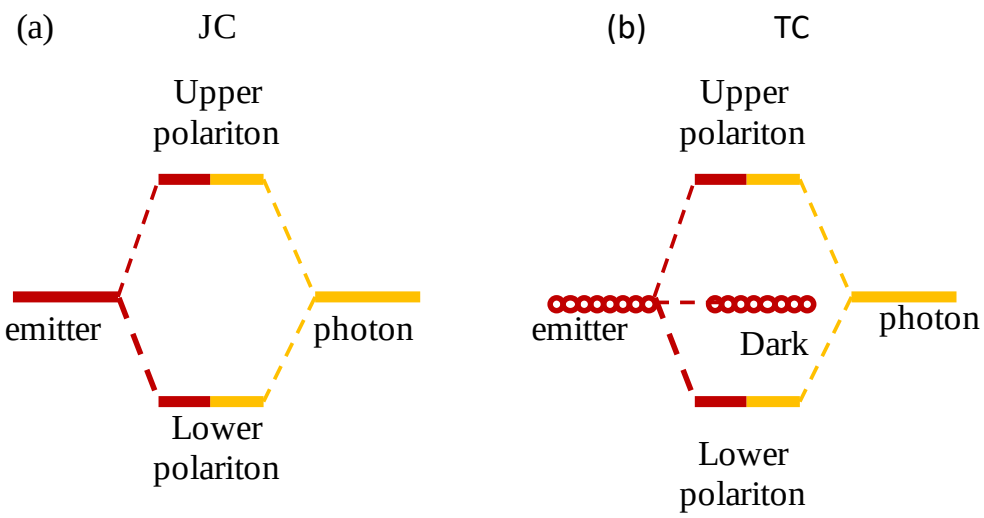

Figure 1.4 (**a**) Schematic of a J-C model and (**b**) T-C model. This figure has been taken from Ref [13]

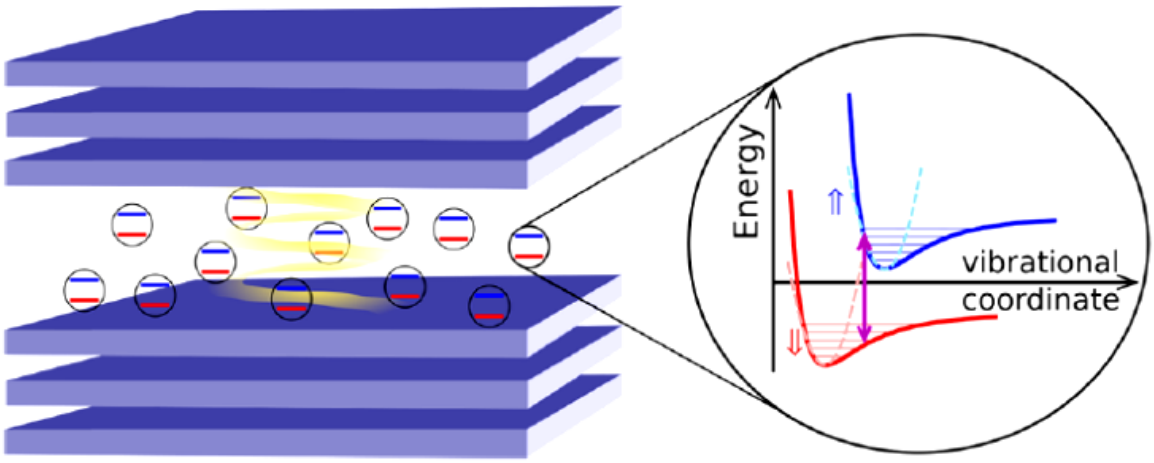

Figure 1.5. N-molecules placed in a cavity represented using Holstein−Tavis−Cummings model, where each molecule is represented by two electronic states, and an associated vibrational mode corresponding to the potential energy surface in the given electronic state. This figure has been taken from Ref[29]

HTC model is given by

$$\hat{H}_{HTC} = \hat{H}_{TC} + \hat{H}_{ph} + \hat{H}_{ex-ph}$$

$$\hat{H} = \omega\hat{a}^{\dagger}\hat{a} + \sum_{i=1}^{N} \omega_0 \hat{\sigma}_i^{+}\hat{\sigma}_i^{-} + \frac{\omega_R}{\sqrt{N}}\left(\hat{\sigma}_i^{+}\hat{a} + \hat{\sigma}_i^{-}\hat{a}^{\dagger}\right) + \omega_{\nu}(\hat{b}_i^{\dagger}\hat{b}_i - \lambda_0 \sigma_i^{+}\hat{\sigma}_i^{-}(\hat{b}_i^{\dagger} + \hat{b}_i))]$$

Annihilation operator, â, represents cavity photon mode which is coupled to the number of molecules (1,2,…., N), where each is represented by two electronic states (Pauli operator σ̂) and vibrational levels by annihilation operator $\hat{b}_i$. In figure 1.6, N emitters in F-Pthe cavity as well as anti-crossing dispersive curve is shown.

The last term in the equation depicts the vibrational coordinate in excited and ground state. ω and ω_0 are the frequencies of cavity and molecular transition respectively whereas ω_R is the Rabi splitting between polaritons formed. The factor λ_0 can be related to the Stokes' shift between absorption and emission spectra in the absence of light matter strong coupling. Total number of photons and electronic excitations are conserved because of Rotating wave approximation.

$$N_{ex} = \hat{a}^{\dagger}\hat{a} + \sum_{i=1}^{N} \hat{\sigma}_i^{+}\hat{\sigma}_i^{-}$$

This implies that $\omega_R < \omega, \omega_0$; which comes hand in many experiments.

1.2.3 ULTRA-STRONG COUPLING REGIME

In strong coupling regime, Rabi splitting is larger than dissipative couplings of cavity but lesser than transition energy. Ultra-Strong Coupling violates above assumption;

$$\frac{\Omega_R}{\omega_c}, \qquad \frac{\Omega_R}{\omega_s} > 10\%$$

Since Rabi splitting is very large compared to parent transition energy, other eigenstates are also perturbed leading to deviation from the behavior seen in light-matter strong coupling.[27] This leads to changes in bulk properties of the material.

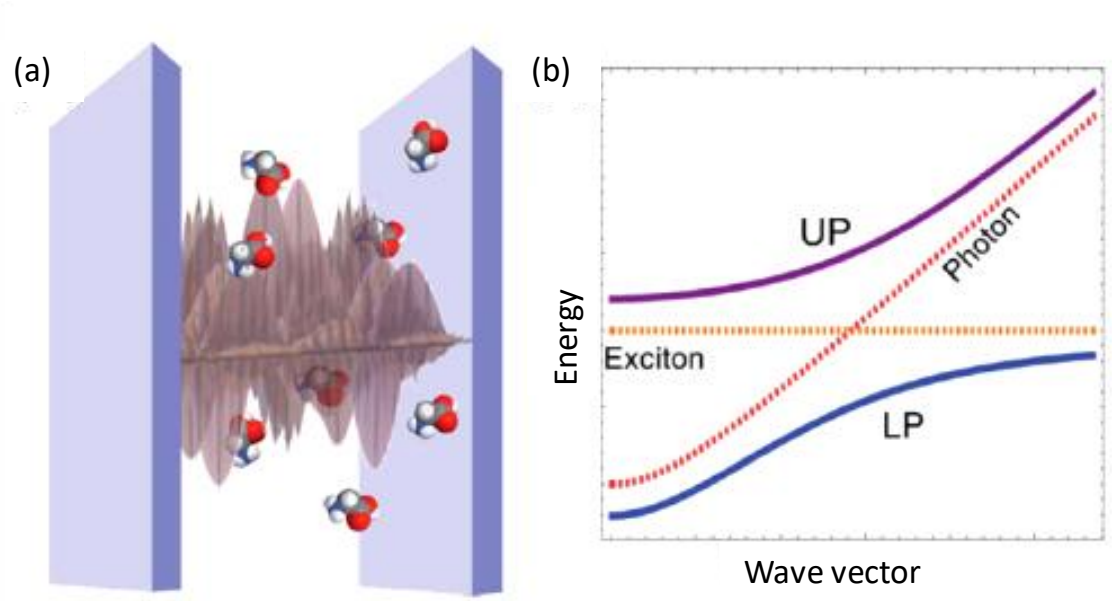

Figure 1.6 (a) Schematic representation of N-molecular emitters embedded in a resonant F-P cavity (b) Cavity, emitter and polariton dispersions generalized using T-C model. Figure is taken from Ref [19].

Ultra-strong coupling was responsible for modification in the work function and phase transition of perovskite material.[30] In strong coupling regime, total excitation number of systems are conserved, but in ultra-strong coupling regime, different excitation number of systems are allowed to hybridize. Lower polariton formed in USC is the superimposition of states consisting of photons and delocalized molecular excitations.

The above description of different regimes of light-matter interactions signifies the modifications that it can bring into the coupled systems. Hence, strong coupling is not only of interest in the field of optics but can be significantly used to modify chemical and physical properties. It can be used as a spectroscopic tool and at the same it can be selectively coupled to vibrational bond that in terms tilt a potential energy surface in favoring a particular reaction than cannot be achieved via any other chemical techniques. In the next chapter, we will discuss about the modification of the vibrational ladder of electronic state by the formation of vibro – polaritonic states and show how an excited state gets affected due to vibrational strong coupling.

CHAPTER II

2.1 INTRODUCTION

2.1.1 SPECTROSCOPY

Spectroscopy is the study of the interaction of electromagnetic radiation with the matter as a function of wavelength (or frequency). In electronic transition, an oscillating electromagnetic field interacts with the transition dipole moment of the molecule, which in principle is being generated by the fluctuation of the electronic cloud. The exchange of energy between the photon and molecules is the heart of such a phenomenon. Photon gives energy hν to excite a molecule from lower excited state E_1 to higher excited state E_2.

Due to the conservation of energy

$$h\nu = E_2 - E_1$$

Solving the Schrodinger equation;

$$H\Psi = E\Psi$$

$$\int \Psi^* H \Psi d\tau = E$$

Ψ is the eigen function of H and E is the corresponding eigen value.

Born-Oppenheimer approximation can be used to separate total wavefunction into the electronic and nuclear part;

$$\Psi_{tot} = \Psi_{el}(q_{el)}\, \Psi_{nucl}(q_{nucl})$$

Ψ_{Nucl} can be further divided into vibrational and rotational parts.

$$\Psi_{tot} = \Psi_{el}(q_{el)}\, \Psi_{vib}(q_{vib})\, \Psi_{rot}(q_{rot})$$

Therefore total energy now becomes;

$$E_{tot} = E_{el} + E_{vib} + E_{rot}$$

Spectroscopic transition is the change of a molecule from one quantum state to another. This transition can be studied by solving time-dependent Schrodinger equation

$$H\Psi = i\hbar\frac{\partial\Psi}{\partial t}$$

Intensity of spectroscopic absorption

$$Intensity \quad \alpha \quad < \Psi^f \left|\mu_z\right| \Psi^i >^2$$

Assuming that electric field is polarised in the z-direction.

For an allowed electronic transition;

$$\int \Psi^f_{el} \mu_\alpha \Psi^i_{el} d\tau_{el} \neq 0$$

Where μ_α is transition dipole moment (TDM) of the molecule.

TDM $\alpha \int \Psi^f_{el} \mu_\alpha \Psi^i_{el} d\tau_{el} \int \Psi^f_{vib} \Psi^i_{vib} d\tau_{vib}$

$$\int \Psi^f_{el} \Psi^f_{vib} \mu^e_\alpha \Psi^i_{vib} \Psi^i_{el} d\tau_{vib} d\tau_{el} \neq 0$$

Which gives vibrational selection rule. Symmetry of molecular eigenstate also needs to be considered for spectroscopic transitions.[32] Vibrational motion of molecules is described using simple harmonic oscillator approximation.

The rate constant for transition between two states are :

$$k_{obs} = k^0_{max} f_e \, X \, f_v \, X \, f_s$$

Where k^0_{max} is the maximum possible rate constant which is defined by zero point motions. f_e , f_v and f_s are the prohibition factors associated with electronic, vibrational and spin configurational changes.

Fermi's Golden rule states that the rate of spontaneous emission depends upon the density of states of the coupled electromagnetic field:

$$k_{obs} \sim \rho [< \Psi_1 |P'_{1\to2}| \Psi_2 >]^2$$

In the above equation, ρ is referred to as the density of states which are the accessible states that can achieve the same energy during the time scale of interaction between the states. $P'_{1\to2}$is the perturbation that takes place in thesystem from $\Psi_1 \to \Psi_2$. As ρ changes, the rate of spontaneous emission changes drastically, which is called as Purcell effect.

Using Fermi's golden rule, we can summarize the rate expression as

$$k_{obs} = \frac{k^0_{max} [< \Psi_1 |P_{vib}| \Psi_2 >]^2}{\Delta E^2_{12}} [< \chi_1 | \chi_2 >^2]$$

Since spin-orbit coupling also affect k_{obs}:

$$k_{obs} = \frac{k^0_{max} [< \Psi_1 |P_{vib}| \Psi_2 >]^2}{\Delta E^2_{12}} X \frac{[< \Psi_1 |P_{SO}| \Psi_2 >]^2}{\Delta E^2_{12}} [< \chi_1 | \chi_2 >^2]$$

The rate of transition is proportional to the square of the product of vibronic coupling matrix element and vibrational overlap element (or Franck Condon factor) .[31]

Rate of spontaneous emission gets enhanced when the molecule is inside a cavity with a resonant photonic mode as photon density ρ is increased inside the cavity than the free space.

As already mentioned, Born- Oppenheimer approximation assumes that nuclear motion is much slower than electronic motion. Franck-Condon principle states that since nuclei are more massive than electrons, the electronic transition takes place from one orbital to another orbital while nuclei remain stationary, which implies that as electronic configuration readjusts from Ψ_1 to Ψ_2, nuclei coordinates remain fixed. Franck-Condon factor or vibrational overlap integral $<\chi_1|\chi_2>$, determines the probability of transition. Potential energy surface with respect to three different situations is shown in Figure 2.1(a). Equilibrium nuclear separation in ground and excited electronic states can be identical, $r_{xy} = r^*_{xy}$, whereas its may not be (r$r_{xy} > r^*_{xy}$) in several

systems as shown in Figure 6(b). In the last situation (Figure 6(c)), equilibrium nuclear separation in excited electronic state is much larger than that of ground electronic state.

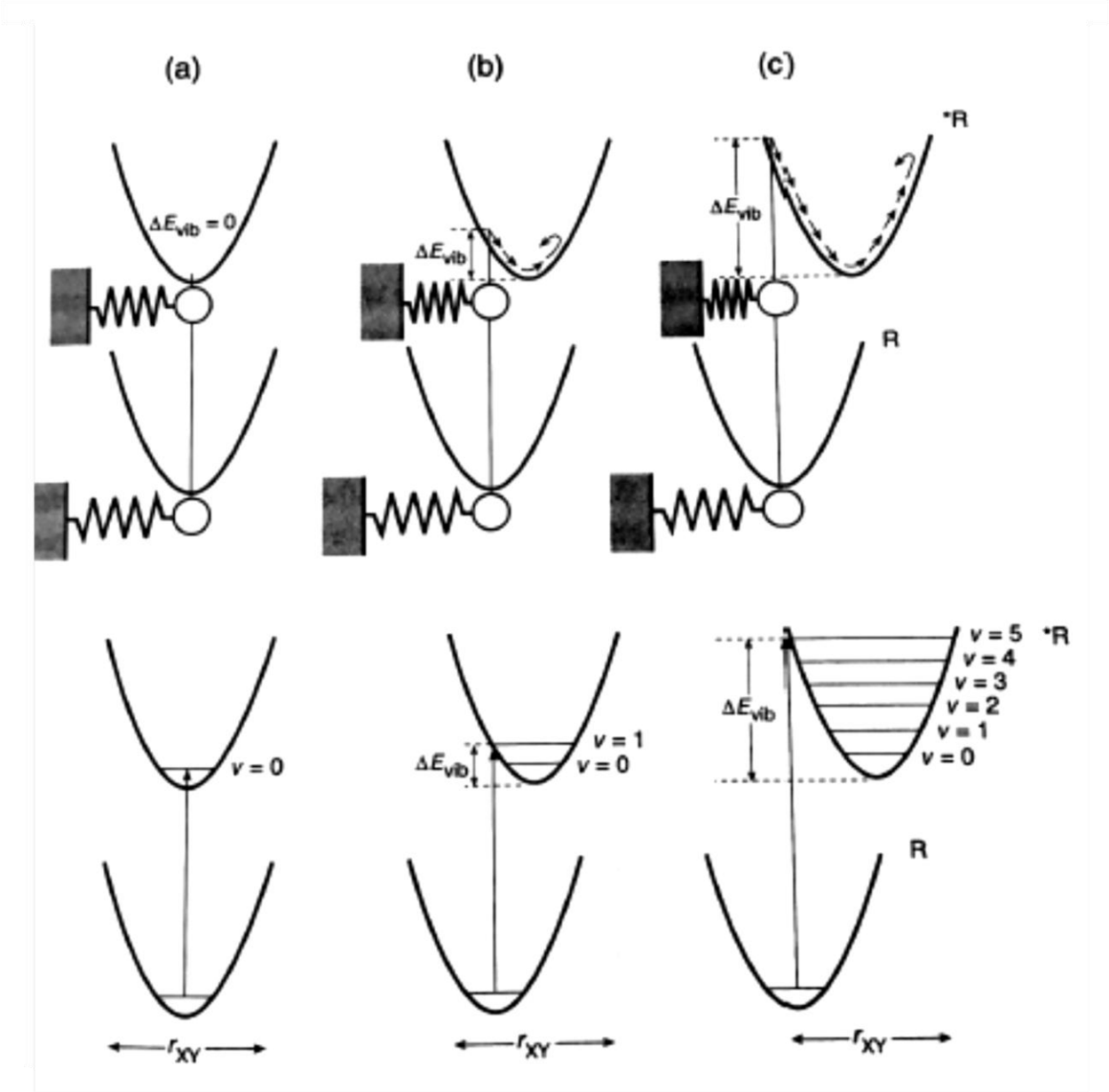

Figure 2.1 (a**)** Representation of F-C principle. Figure has been taken from Ref [33]

Figure 2.1 also highlights that transitions are vertical as nuclear coordinates are supposed to be stationary. F-C principle provides selection rule for vibronic transitions, magnitude of integral $< \chi_1 | \chi_2 >$ determines the probability of transition.

Oscillator strength that measures the probability of electronic transition induced by electromagnetic field, $f = 4.3\ X\ 10^{-9} \int \varepsilon\, d\bar{v}$

Oscillator strength, $f\ \alpha\, \mu_i^2\ = (er)^2$ Transition dipole moment

Electronic absorption spectrum depends upon two important laws: Beer's and Lambert's laws::

Lambert's law states that the proportion of light absorbed by medium does not depend on initial light intensity. Beer's law states that the amount of light absorbed depends upon the concentration of molecules and pathlength of light.

Optical density, $OD = \log\,(I_0/I_t)$

$\varepsilon = [\log(I_0/I_t)]l[A]$,

I_0 and I_t are intensities of incident and transmitted light, L is the pathlength and [A] is the concentration. Both absorption and emission spectra reflect the vibrational ladder of a given potential energy surface.

2.1.2 SYSTEM UNDER STUDY: 1,3 DIKETONES

β-Dicarbonyl compounds have been of great interest to organic, inorganic and physical chemists. In inorganic chemistry, β-dicarbonyl compounds have been used extensively to study chelate chemistry. Physical chemists use 1,3 diketones to study keto –enol equilibrium. Scientists like Kuo, Veirov et al. and Markov et al. were interested in the study of such neutral molecules due to the possibility of proton migration in a double well potential.[42-46] Enol forms are often favored over keto tautomers because of intra-molecular hydrogen bond that stabilizes enol forms.

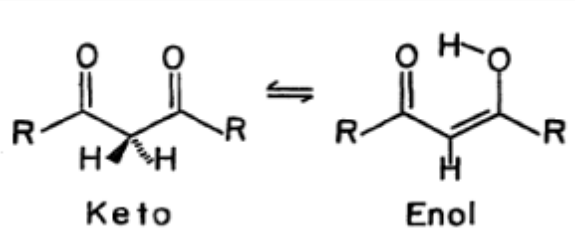

Figure 2.2: Keto-enol tautomerisation of 1,3 diketone

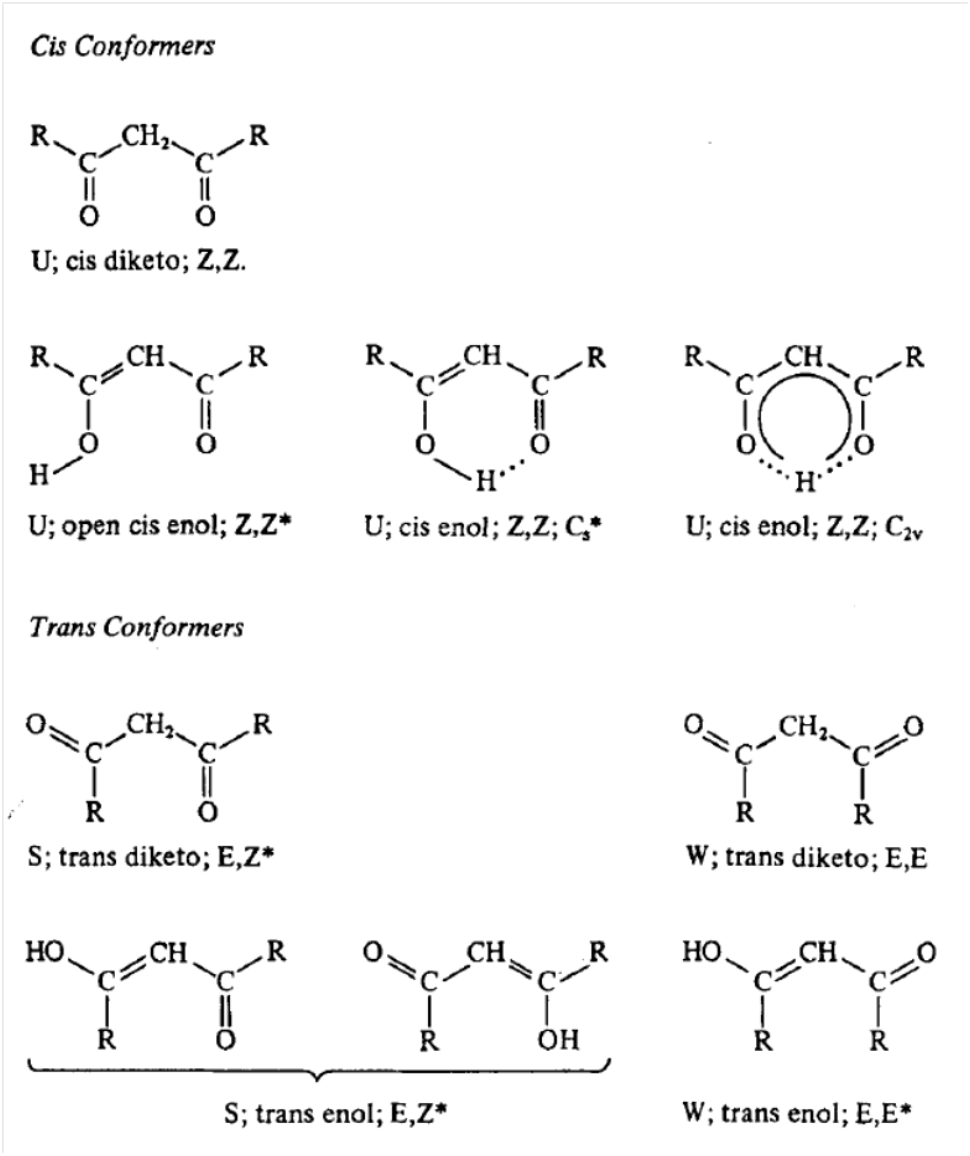

Figure 2.3 shows conformers that are possible for β-diketones. This figure was taken from Ref [42]

The formation of chelate ring (Figure 2.2) is the primary feature of such molecules. There were lots of debate regarding the chelate structure of diketones, for example in case of dibenzoylmethane Morton et al. showed that it exists in unchelated enol form.[39] But later it was showed by Hilbert and co-workers that it also exists in chelated form.[40] Different conformers possible for 1,3 diketones are shown in Figure 2.3.

Extremely rapid proton transfer from one oxygen in cis-enol tautomer to the trans-form is possible, due to the presence of two minima of asymmetrical double well potential as shown in Figure 2.4. This phenomenon in which particle can escape through the barrier is known as tunneling effect. [36]

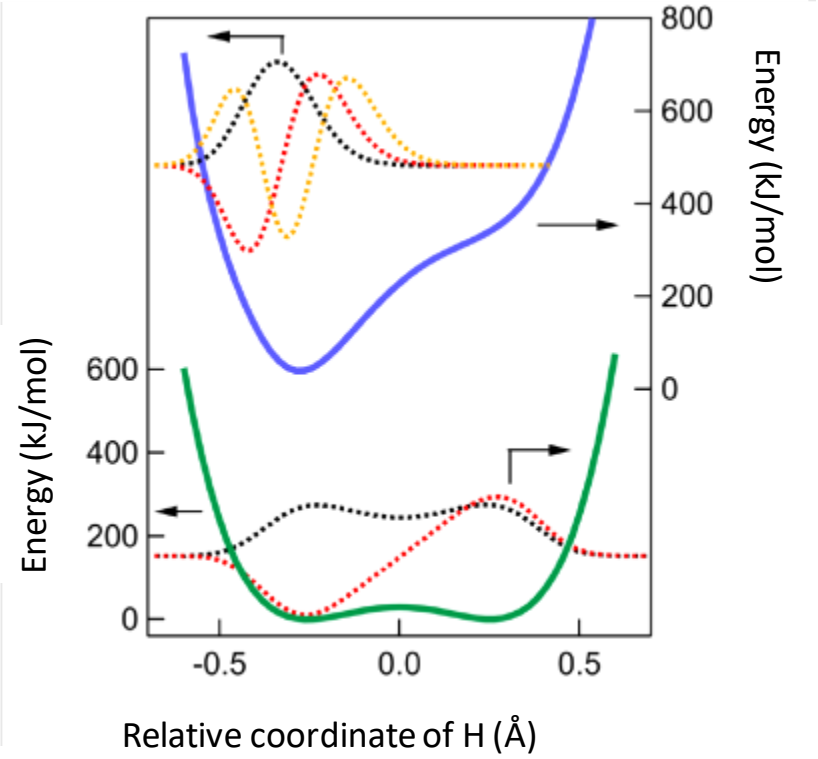

Figure 2.4 Simulation is showing the ground and excited state of acetylacetone by varying O-H bond distance. This figure has been taken from Ref [36]

The percentage of enol tautomer depends upon many factors like solvent, temperature, inter-molecular hydrogen bonding, etc. Lower the polarity of the solvent, higher will be the percentage of enol tautomer.[42] As temperature increases, the amount of enol tautomer decreases. For

simplest β-diketone, malondialdehyde, Seliskar et al. identified two? electronic transitions where they have assigned the peak at 300nm to be that of $n \rightarrow \pi^*$ and at 263 nm to that of $\pi \rightarrow \pi^*$.[34] The O-H stretch and C=O vibrational band indicate that the strength of intramolecular hydrogen bonding varies in the order- acetylacetone < benzoylacetone < dibenzoylacetone.

We have chosen an asymmetric β-diketones for our experiment with intention of having distinguished vibrational bands for both keto and enol forms. These molecules also exhibit strong intramolecular hydrogen bonding (>10 kJ/mol), VSC can control the equilibria and hence the spectroscopic properties of the system. [35]

2.2 EXPERIMENTAL METHODS

1-Phenyl 1,3 butanedione(benzoylacetone) is purchased from Sigma-Aldrich. IR spectrum of the molecule in gaseous and solution phase is shown in Figure 2.5 b and c. Benzoylacetone has vibrational stretches at 1715cm^{-1} and 1695 cm^{-1} corresponding to carbonyl stretches of methyl and phenyl groups respectively. It also has a carbonyl stretch corresponding to enol group at 1605cm^{-1}.

At first, solution of benzoylacetone was prepared in cyclohexanone (spectroscopic grade) Cyclohexanone was chosen due to the availability of a strong vibrational band at 1715 cm^{-1} as shown in Figure 2.5(b). This combination will help us to have a co-operative interaction in the system by simply coupling both the solvent and the solute vibration to an IR cavity mode. The co-operativity effect increases the collective Rabi splitting as Rabi splitting is proportional to the square root of number of molecules and thus intensifies the local effect per molecules coupled to the IR photon. Stock solution of benzoylacetone (0.01M; BOA) in cyclohexanone (CyHxO) was prepared and most of the VSC studies were done with this combination of solvent-solute mixture-unless otherwise will be mentioned in the respective session.

Different solutions of BOA in CyHxO were prepared by diluting stock solution to vary concentration and verify Beer – Lambert's law in the non-cavity as shown in Table 2.1. UV-Vis spectra of each of the solutions were recorded. Absorbance at λ_{max} of both keto and enol.

tautomer were noted down and plotted against the concentration. UV-Vis spectra and IR spectra were recorded using a liquid sample cell set (Figure 2.6(b)) obtained from Specac.

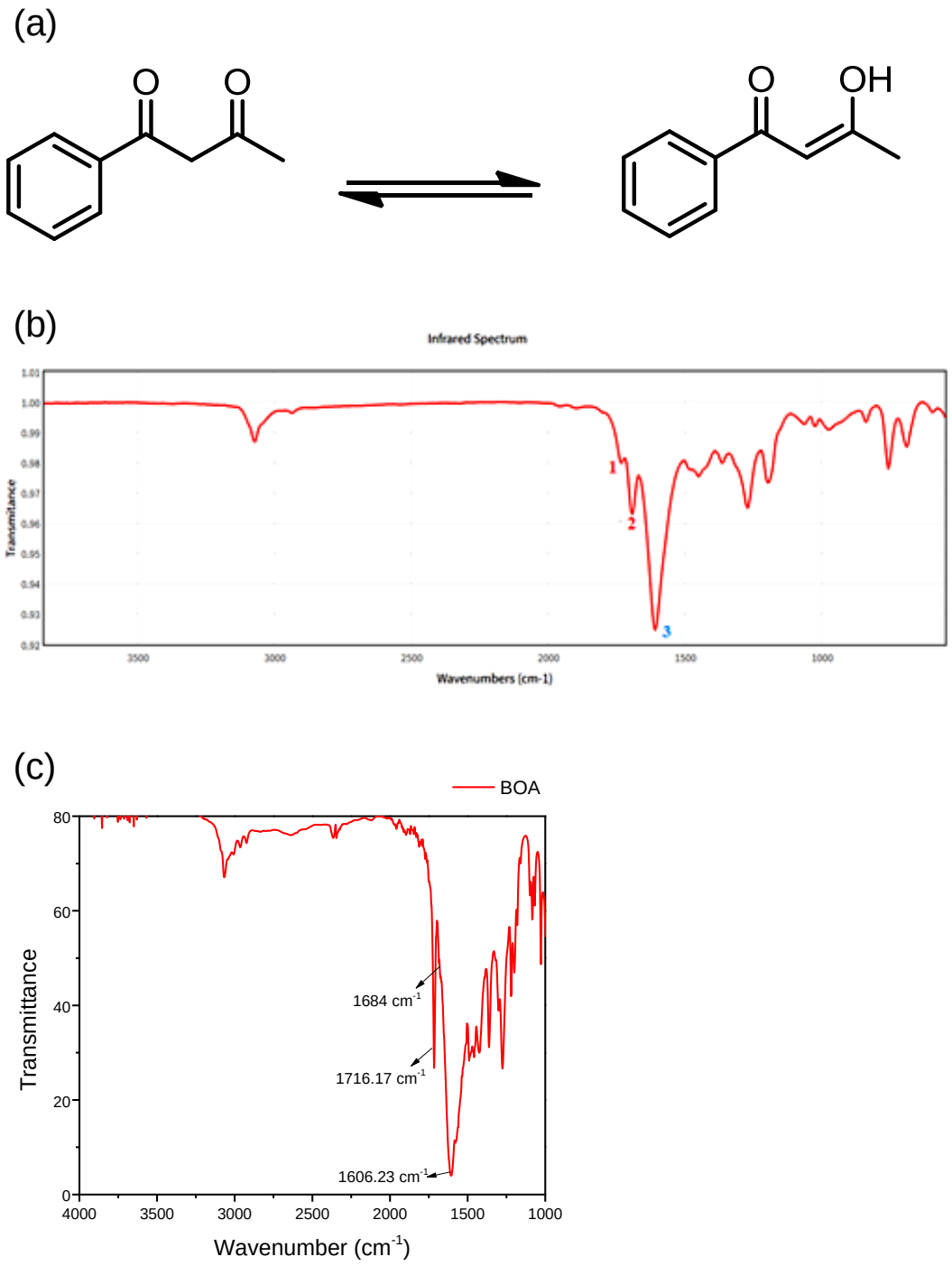

Figure 2.5: IR spectra of BOA (b) gas phase and in (c) solution phase

Table 2.1

Volume of CyHxO (μL)	Volume of 0.0123M BOA in CyHxO (μL)	Final Molarity (M)
100	100	0.00615
100	233	0.0086
100	300	0.0093
100	400	0.0098

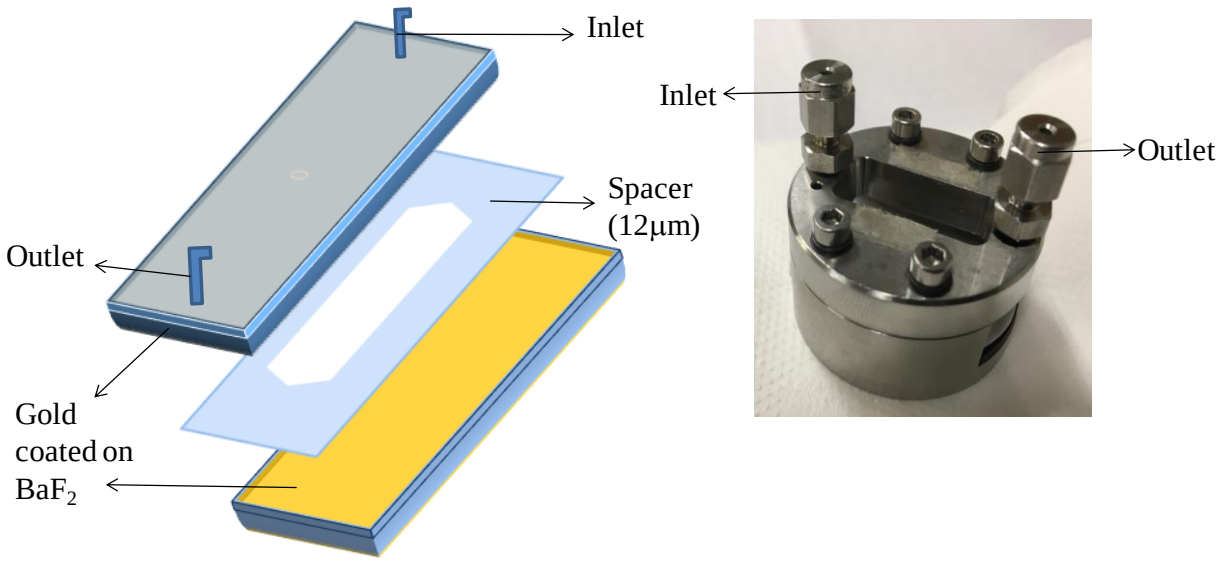

Figure 2.6 (a) Schematic representation of the F-P cavity (b) shows the corresponding cavity used for the experiment.

Data collection in non-cavity was obtained by injecting sample through inlet into the microfluidic cell as shown in Figure 2.6. Inside the cell, BaF_2 windows are normally used substrate which are separated by a spacer of 12μm. Using Beer-Lambert's law:

$$Abs = \varepsilon cL,$$

(where ε is the molar extinction coefficient, c is the concentration of the solution, and L is the pathlength) molar extinction coefficients for both keto and enol tautomer were calculated from absorbance vs. concentration plots. The baseline for UV spectra was recorded by injecting solvent cyclohexanone into the cavity in which one of the modes is tuned to be at 1715 cm^{-1} as shown in figure 2.7(b).

The same experiment was repeated in the F-P cavity to verify Beer-Lambert's law in the cavity. F-P cavity was produced by sputtering 10 nm of gold on top of BaF_2 windows which are separated by Mylar spacers as shown in Figure 2.6(a). Mylar spacers determine the pathlength of the system. Mylar spacers are selected depending upon the vibrational mode to be coupled. For this experiment, we have chosen 6, 12 and 18 μm spacers.

After measuring baseline, BOA in CyHxO is injected into the cavity; modes are tuned from 1700cm^{-1} to 1850cm^{-1}. Absorbance at λ_{max} corresponding to both keto and enol tautomer is measured at each value of tuned cavity mode. These values were then used to plot Absorbance vs. pathlength/wavenumbers which can be assessed by getting the FSR of the higher order cavity modes, similar set of experiments were conducted by VSC with different cavity modes and details are presented in the next section.

2.3. RESULTS AND DISCUSSIONS

We started the experiment to see the effect of strong coupling on the equilibrium constant for the keto-enol tautomerism. Negligible change in the equilibrium was observed under VSC of the solvent molecule. This can be due to strong intramolecular H-bonding present in BOA. A closer analysis of the UV-Vis studies showed interesting deviation from linear behavior of absorption of BOA in the IR cavity. Then we persuaded further studies by systematically looking into n-pi* and pi-pi* transition in BOA.

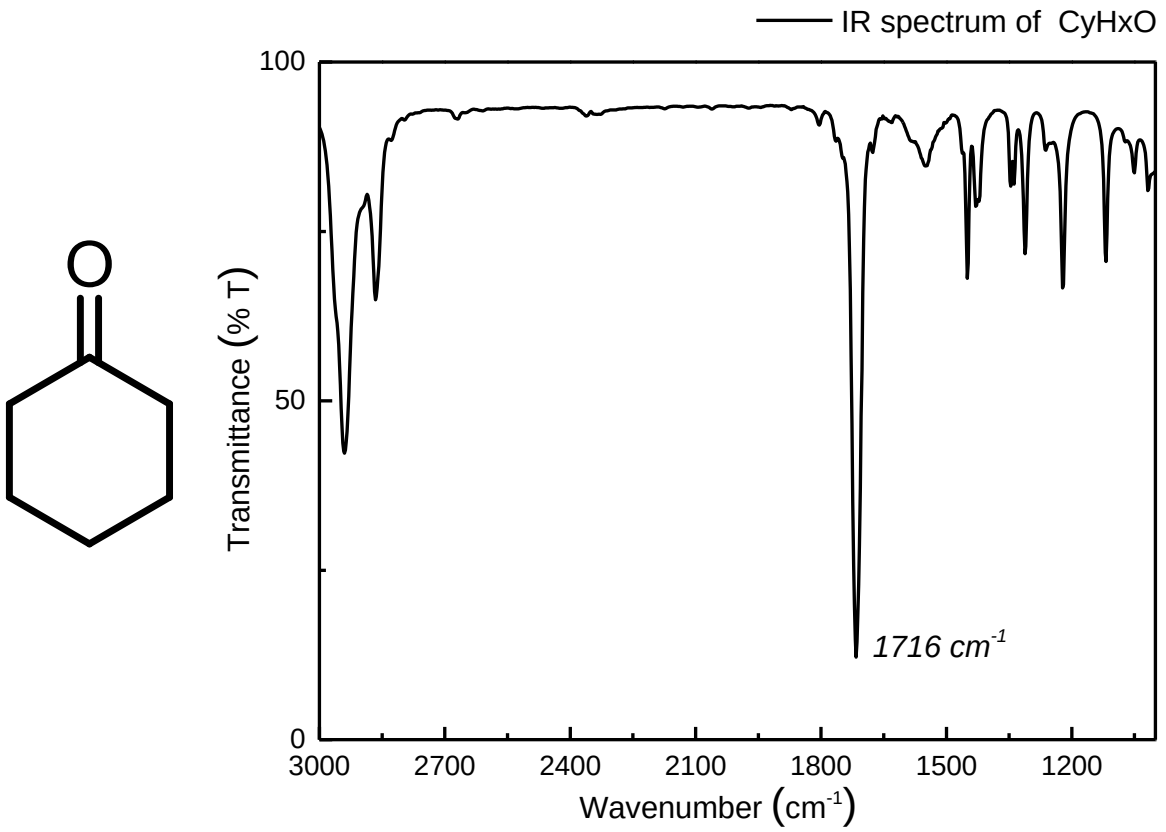

Figure 2.7 Infrared spectrum of cyclohexanone

2.3.1 ABSORPTION STUDIES IN NON-CAVITY (MICROFLUIDIC CELL)

Ultraviolet absorption spectra for the solution BOA in CyHxO in non-cavity is shown in Figure 2.8(a), from where $\lambda_{max}$of keto tautomer at 250 nm and that of enol tautomer at 311 nm. Pathlength is fixed at 12 μm. Data are plotted by taking absorbance (λ_{max}) vs concentration of the solution both in non-cavity and cavity conditions. Linear plots are obtained for both enol and keto tautomer as shown in Figure 2.8(b) and (c).

The result (Figure 2.8)show that in non-cavity condition Beer – Lambert's law that is obeyed for both keto and enol molecular transitions.

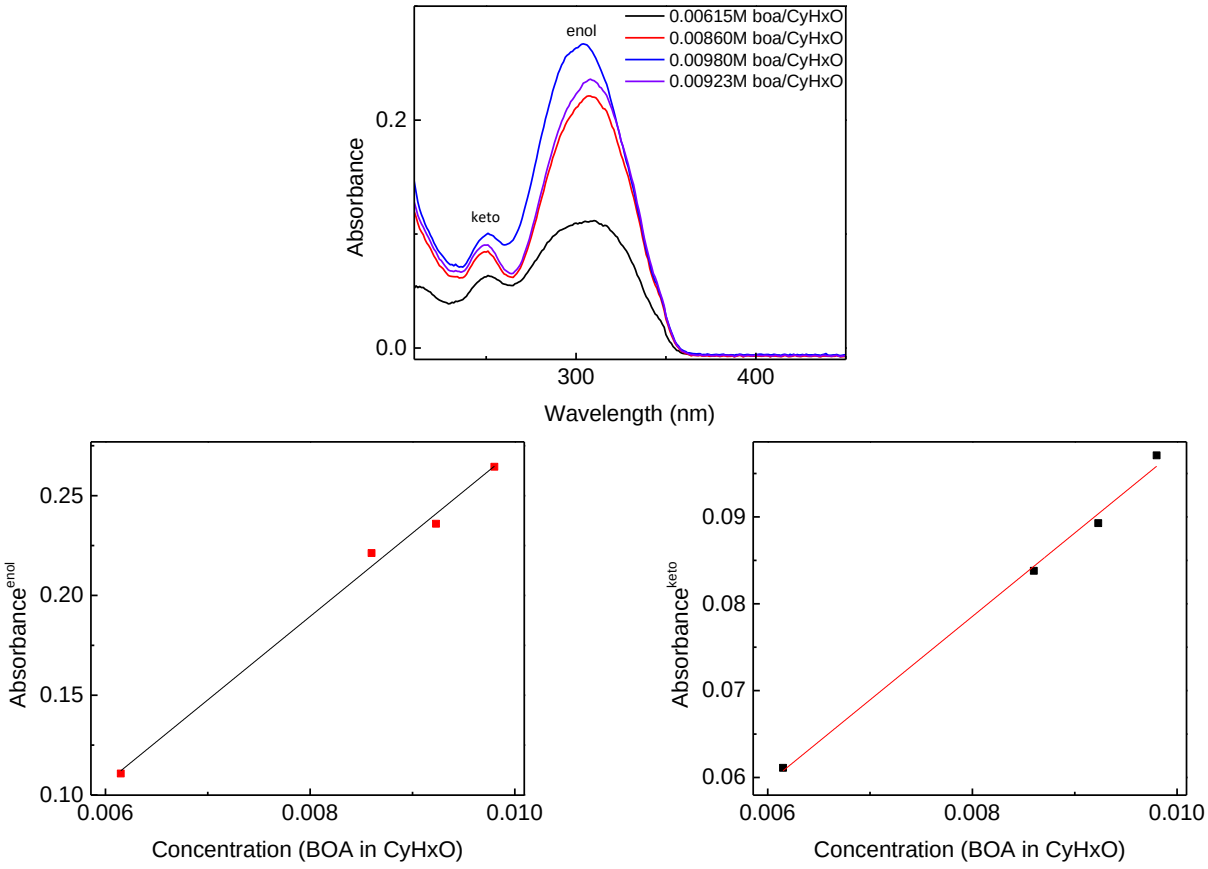

Figure 2.8(a) UV absorption spectrum of BOA in CyHxO (varying concentration). $\lambda_{\max}^{keto}$ = 250 nm and $\lambda_{\max}^{enol}$ = 310 nm. (b) Linear absorbance vs. concentration plots for both keto and (c) enol

2.3.2 ABSORPTION STUDIES UNDER VSC

F-P cavity is tuned by moving the top mirror systematically, cavity modes frequencies are changed accordingly. This result in getting a full picture of the absorbance variation under ON as well as OFF-resonance conditions. Chosen molecule has characteristic vibrational bands at 1715cm^{-1}, 1698 cm^{-1} and 1605 cm^{-1}.

First we studied the system by coupling methyl carbonyl stretch which is at 1715 cm^{-1}, cavity mode was tuned such that one of the cavity modes was set to be at 1715 cm-1 to be ON resonance.

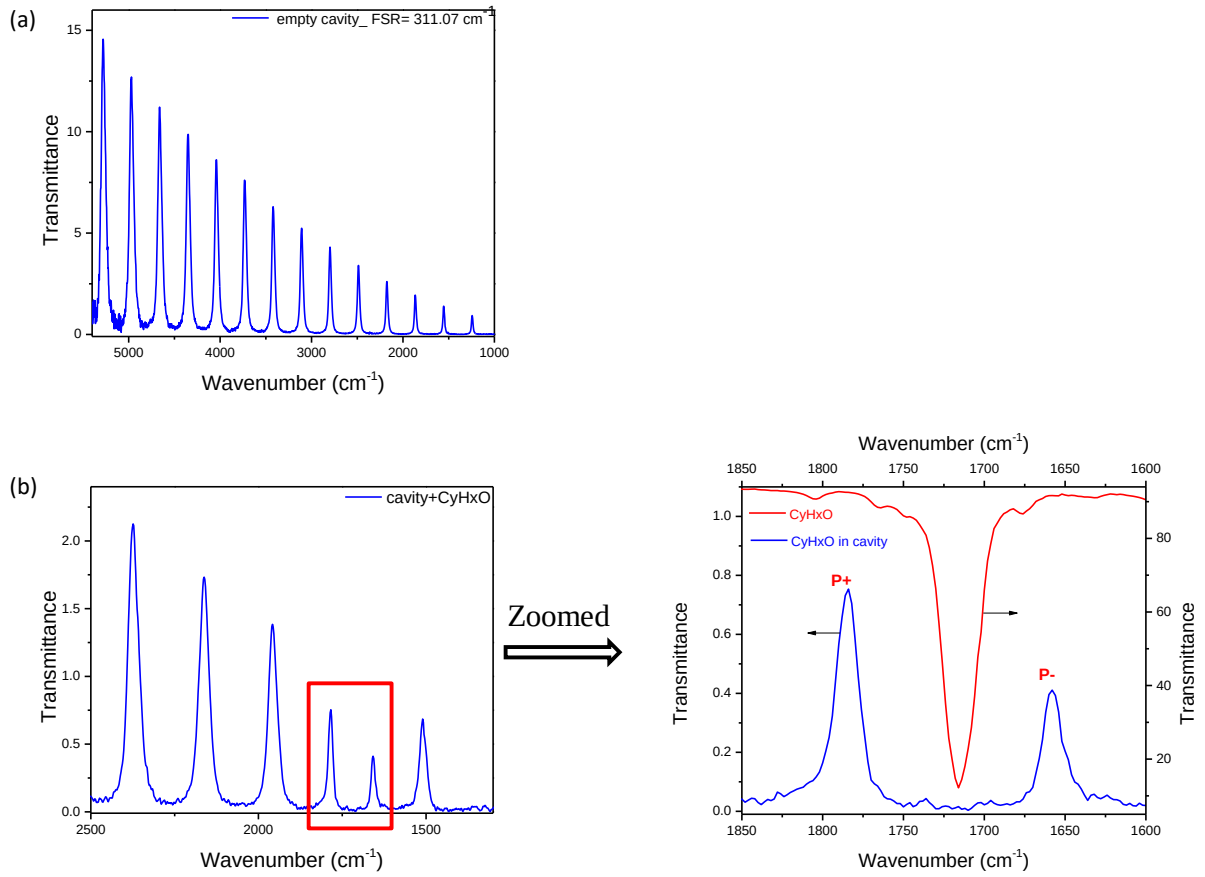

Figure 2.9 (a) shows empty cavity tuned at 311 cm^{-1} (b) shows vibro – polaritons formed because of coupling between carbonyl stretch at 1715cm^{-1} and resonant cavity mode which is zoomed further in the appropriate region.

Actual cavity mode position can be predicted if the refractive index of the injecting medium is known, which follows a relation,

$$k = \frac{10^4}{2nL}$$

where k is the free spectral range (FSR), n is the refractive index and Lis the spacing between the two mirrors.

The empty cavity was set at 311.07 cm^{-1} according to the calculations as shown in figure 2.9(a).

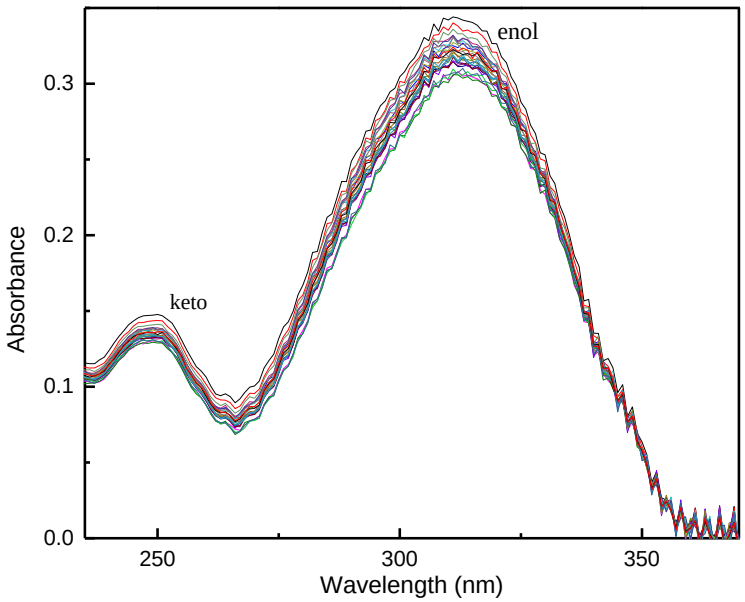

Figure 2.10 shows UV spectra recorded BOA/CyHxO in the cavity. UV spectra are recorded for cavity modes such that they are tuned from 1700 cm^{-1} to 1850 cm^{-1}.

FSR was tuned such that cavity mode is changing from 1700cm^{-1} to 1850cm^{-1}. UV spectra for each tuned cavity are recorded and plotted as shown in Figure 2.10.

Absorbance of enol tautomer at $\lambda_{\max}^{enol}$ = 310 nm vs. pathelength(in wavenumbers) was plotted so as to verify Beer-Lambert's law as shown in Figure 2.11. Spacer of 12 μm was used and 8th cavity mode was coupled to the vibrational band of BOA at 1715 cm^{-1} corresponding to methyl carbonyl stretch. Unlike in non-cavity, we observed a non-linear behavior in Beer-Lambert's law by VSC. Sharp oscillations were observed when the cavity mode crosses the vibrational envelope.

The same experiment was repeated using different spacers: 4th and 12th cavity modes were coupled to the vibrational band of BOA for 6 and 18 μm spacers, respectively. Corresponding absorbance of enol tautomer at $\lambda_{\max}^{enol}$ = 310 nm vs. pathelength (in wavenumbers) plots are shown in Figure 2.12.

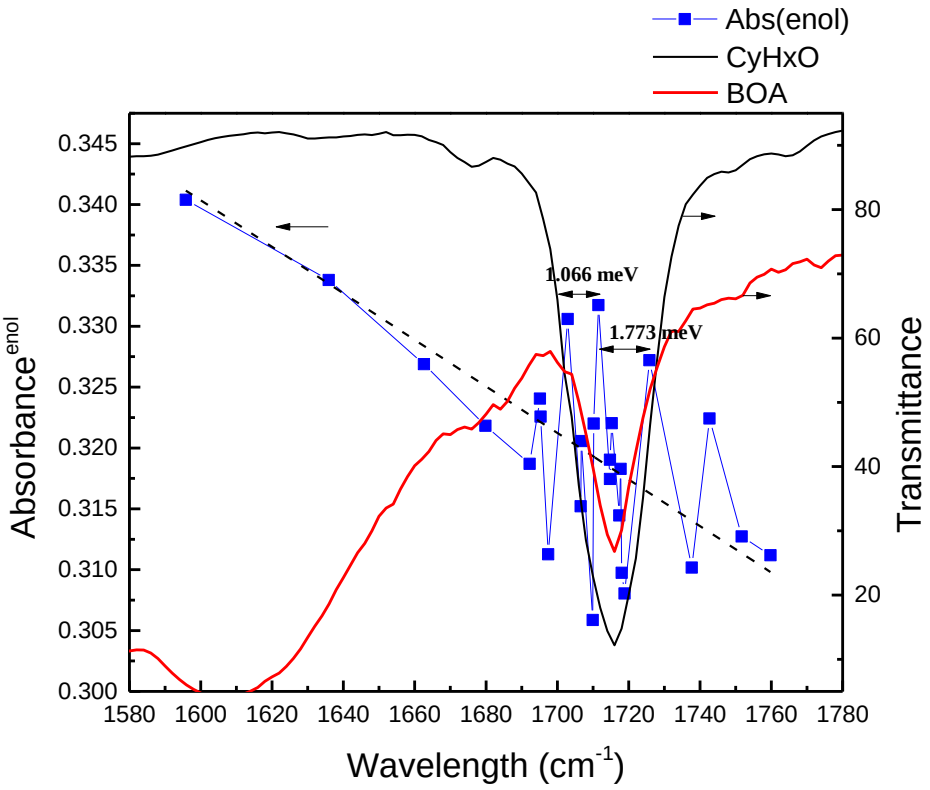

Figure 2.11 Blue plot corresponds to the plot of absorbance of enol tautomer at $\lambda_{\max}^{enol}$ = 310 nm vs. pathelength(in wavenumbers). IR spectra of Cyclohexanone and BOA in solution phase (spacer: 12 μm).

As shown in Figure 2.12, three sets of data are shown. Set I and II correspond to the cavity in which 6 and 12 μm spacers are used. Similar to the results obtained before, sharp fluctuations from Beer-Lambert's law is observed. a Interestingly, Set III, a spacer which give 12th cavity modecoupling show negligible changes in the absorbance variations.

We have further analysed the data to see any periodicity arising the in the absorbance variation

To our surprise, both 4th and 8th modes gave completely different pattern and cannot be directly linked to any frequency variation in the system.

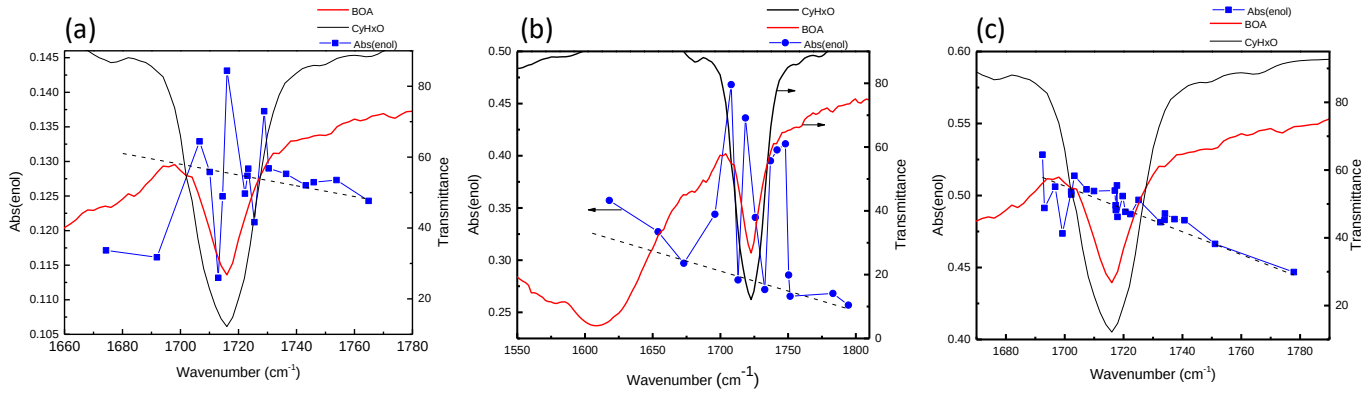

Figure 2.12 Absorbance vs wavenumber (blue solid dot-line) plot for VSC of BOA in Cyclohexanone for;(a) 6 μm (b) 12 μm (c) 18 μm spacers.. IR absorption spectra of Cyclohexanone (black solid line)and BOA (red solid line) in solution phase is shown for further comparison.

It is clear from the above tuning experiments that not only the ON resonance condition show the fluctuation, whereas, slowly moving the cavity across the vibrational envelope resulting a shift change in the absorbance due to VSC. It is also observed that spacing between fluctuations are in the order of 1 meV to 2.5 meV.

TABLE 2.2 Spacing between the oscillations observed in absorbance vs. pathlength plot.

Spacer (μm)	**Cavity mode**	**Spacing b/w 1 and 2**		**Spacing b/w 2 and 3**	
		(cm^{-1})	**(meV)**	(cm^{-1})	**(meV)**
6	4	9.5	**1.178**	13	**1.49**
12 (a)	8	8.6	**1.066**	14.3	**1.773**
12 (b)	8	10	**1.24**	19	**2.36**
18	12	-	-	-	-

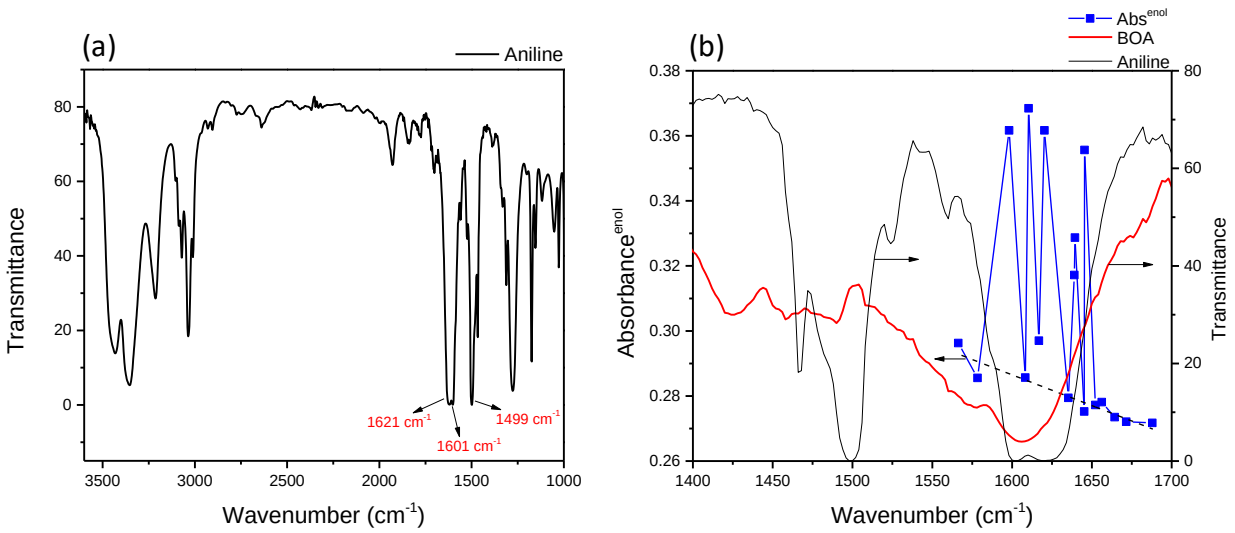

Figure 2.13(a)IR spectrum of solvent aniline (b) Blue plot corresponds to the plot of absorbance of enol vs. pathlength (in wavenumbers). IR spectra of **aniline** and **BOA**

Obtained results were further verified by coupling the carbonyl stretch of enol tautomer which is at 1605cm^{-1}. Another solvent, Aniline which has a NH_2 bending at 1605 cm^{-1} was chosen as solvent to bring in co-operativity effect. A similar protocol was followed; the baseline was measured by coupling NH_2 bending of aniline at 1605cm^{-1} to cavity mode. Solution of BOA in aniline was injected and the cavity was tuned from 1550 cm^{-1} to 1700cm^{-1} · IR spectrum of aniline (Figure 2.13(a)) NH_2 bending at 1605 cm^{-1}overlaps with the carbonyl stretch of the enol tautomer. When vibrational band corresponding to the carbonyl stretch in enol tautomer is coupled, oscillations were observed similar to ones observed when methyl carbonyl stretch was coupled to the cavity mode. Absorbance vs pathlength is plotted in Figure 2.13(b). As the cavity mode overlaps the envelope of the vibrational band, non-periodic fluctuations are observed.

We have conducted another control experiment using carbontetrachloride (CCl_4) as the solvent which doesn't have any vibrational band in the region of benzoylacetone. BOA in CCl_4solution was injected into the F-P cavity, and similar tuning experiment was conducted to verify results. In contrast to the previous experiments, we observed that absorbance at λ_{max} of enol vs. pathlength (in wavenumbers) is more or less a straight line (fluctuation are not pronounced and are within the limit of measurement) as plotted in Figure 2.14. This ensures that cooperativity effect is not operating in the current experiment.

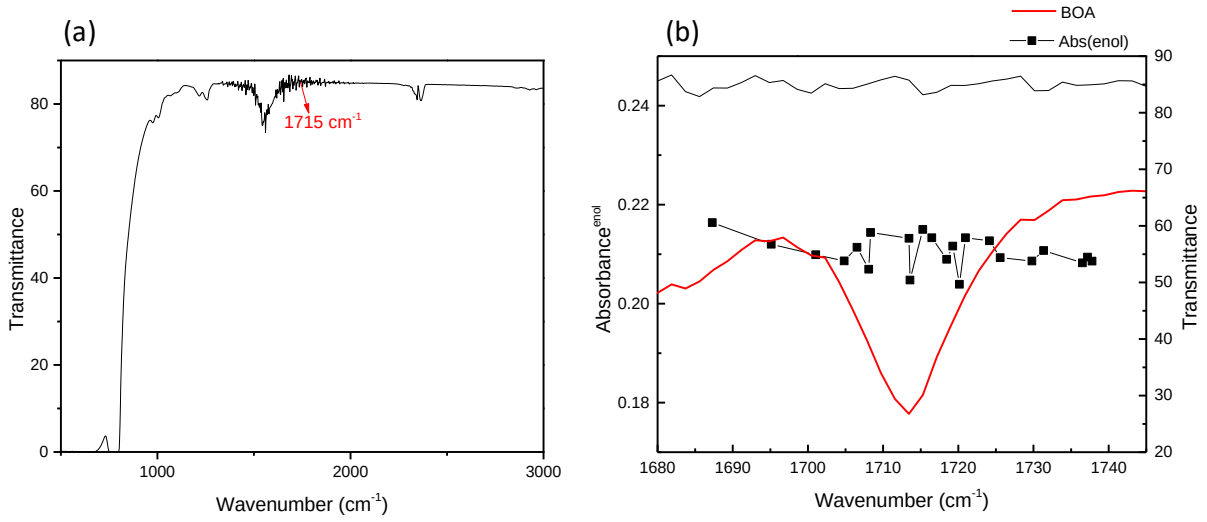

Figure 2.14 (a) IR spectrum of tetrachloride. (It does not have any peak at 1715 cm^{-1}). (b) Black dotted plot shows the plot of absorbance vs. pathlength (in wavenumbers). IR spectra of carbon tetrachloride and BOA.

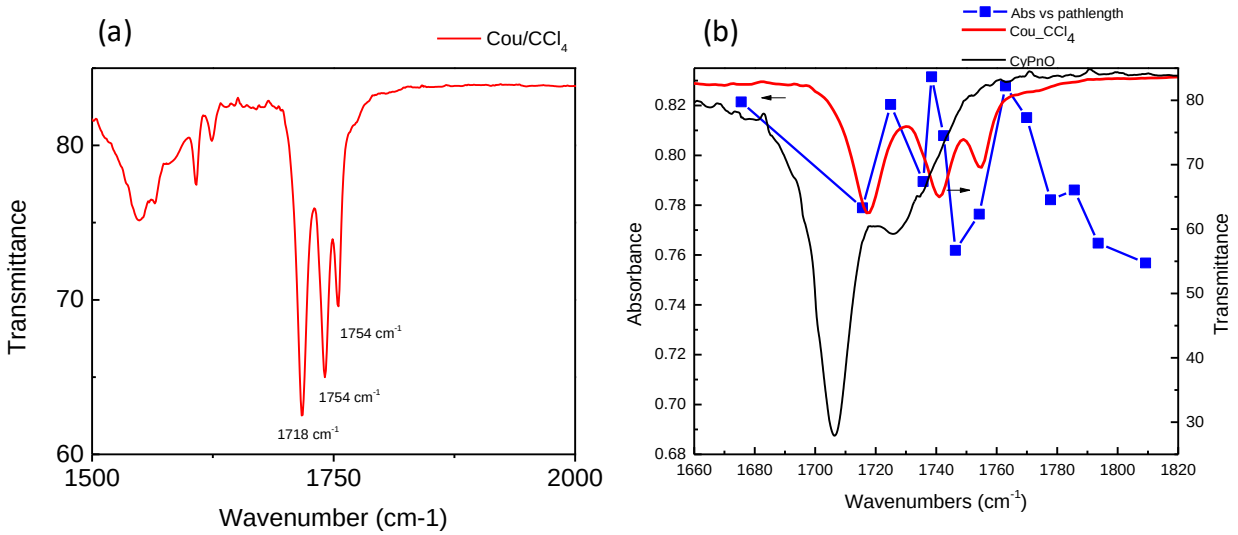

Figure 2.15(a)IR spectrum of coumarin in solution phase (b) Blue plot corresponds to the plot of absorbance vs. pathlength (in wavenumbers).

2.3.2 ABSORPTION STUDIES OF COUMARIN UNDER VSC

To generalize the results obtained, we have taken a well-known chromophoric dye - coumarin-in which the photophysics are known and also have simple energy levels compared to diketones. Coumarin has carbonyl stretches at 1718 cm^{-1}, 1742 cm^{-1} and 1754 cm^{-1} as shown in Figure 2.15(a). Cyclopentanone was chosen as a solvent to bring in the concept of co-operativity effect as it has intense carbonyl stretch at 1750 cm^{-1}. Vibrational band in coumarin was coupled to the 7^{th} mode corresponding to a pathlength of 12 μm was used for the studies. Absorbance vs. pathlength was measured and plotted. A clear deviation of Beer-Lambert's law is observed under VSC of coumarin in cyclopentanone.

CONCLUSIONS

In conclusion, we have seen a clear solvent-solute (cyclohexanone/pentanone-diketone/coumarin system) interaction that was coordinated by VSC by overlapping vibrational states in an electronic reaction co-ordinate. Non-cavity absorption measurements and other control experiments clearly show the existence of vibrational coupling in the ground state of the reaction co-ordinate. However, less is known about the modification of the excited state vibrational energy level.

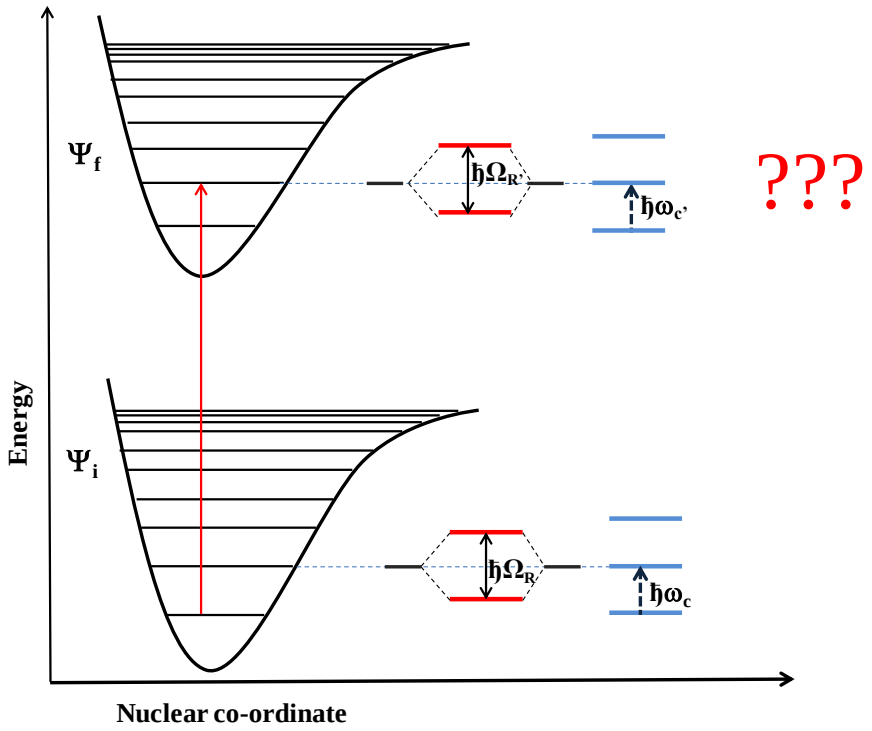

Figure 2.16 Proposed scheme for the changes in the vibrational ladder of ground and excited state under VSC.

Excited vibrational states are non-populated and cannot be coupled to an IR cavity mode directly due the absence of any vibrational dipole. Very interestingly, bringing a solvent vibrational state matching to the frequency of the excited state Franck-Condon (F-C) state here, v_1' state and couple to the same IR photon (IR cavity photon cannot distinguish different oscillators, but only consider the phase and frequency) can generate vibro-polaritonic states with enough separation to see per molecule splitting (2.16). This fundamental change in the vibrational frequency and

also the reshuffling of the wavefunction of v_1' state modify the F-C transition and hence could affect the electronic transition dipole moment of the system. Tuning experiments clearly see the fluctuation behavior, whereas, these fluctuation behaviors are not periodic in the wavenumber frame. Possibly the fluctuation can be periodic in the phase of the system. Here, after strong coupling, vibro-polaritonic states gives a linear combination of all the possible mixing of IR photon of the cavity and vibrational state of the molecule. For e.g., 4^{th} cavity mode (3 nodes) and v_1' state (1 node) result in 3 linear combination of standing vibrational wave pattern. One or more of the patterns will serve as F-C state and reshape depending upon the tuning of the cavity condition. Rigorous theoretical studies are required to understand this most interesting fundamental phenomena.

BIBLIOGRAPHY

[1] T. Hummer, F. J. Garcıa-Vidal, L. Mart´ın-Moreno, and D. Zueco, "Weak and strong coupling regimes in plasmonic QED", *Physical Review B* 87, 115419 (2013)

[2] V. Yakovlev, V. Nazin, and G. Zhizhin, "The surface Polariton splitting due to thin surface film LO vibrations", *Opt. Commun*. 15, 293 –295 (1975)

[3] Y. Kaluzny, P. Goy, M. Gross, J.-M. Raimond, and S. Haroche, "Observation of self-induced Rabi oscillations in two-level atoms excited inside a resonant cavity: the ringing regime of superradiance", *Phys. Rev. Lett*. 51, 1175 (1983).

[4] C. Weisbuch, M. Nishioka, A. Ishikawa, and Y. Arakawa, "Observation of the coupled exciton-photon mode splitting in a semiconductor quantum microcavity", *Phys. Rev. Lett*. 69, 3314–3317 (1992).

[5] A. Wallraff, D. I. Schuster, A. Blais, L Frunzio, R.-S. Huang, J Majer, S Kumar, S. M. Girvin, and R. J. Schoelkopf, "Strong coupling of a single photon to a superconducting qubit using circuit quantum electrodynamics", *Nature*, 431, 162–167 (2004).

[6] T. Schwartz, J. A. Hutchison, C. Genet, and T. W. Ebbesen, "Reversible switching of ultrastrong light-molecule coupling", *Phys. Rev. Lett*. 106, 196405 (2011).

[7] J. A. Hutchison, T. Schwartz, C. Genet, E. Devaux, and T. W. Ebbesen, "Modifying chemical landscapes by coupling to vacuum fields", *Angew. Chem., Int. Ed*. 51, 1592–1596 (2012).

[8] A. Shalabney, J. George, J Hutchison, G. Pupillo, C. Genet, and T. W. Ebbesen, "Coherent coupling of molecular resonators with a microcavity mode", *Nat. Commun*. 6 (2015)

[9] Atef Shalabney, Jino George, Hidefumi Hiura, James A. Hutchison, Cyriaque Genet,

Petra Hellwig, and Thomas W. Ebbesen, “Enhanced Raman Scattering from Vibro-Polariton Hybrid States”, *Angew chem*. 54, 7971 –7975 (2015).

[10] J. George, A. Shalabney, J. A. Hutchison, C. Genet, and T. W. Ebbesen, “Liquid-phase vibrational strong coupling”, *J. Phys. Chem. Lett*. 6, 1027–1031 (2015)

[11] A. Thomas, J. George, A. Shalabney, M. Dryzhakov, S. J. Varma, J. Moran, T. Chervy, X. Zhong, E. Devaux, C. Genet, J. A. Hutchison and T. W. Ebbesen, “Ground-state chemical reactivity under vibrational coupling to the vacuum electromagnetic field”, *Angew. Chem*., 128, 11634 (2016).

[12] Hidefumi Hiura, Atef Shalabney, Jino George, “Cavity Catalysis –Accelerating Reactions under Vibrational Strong Coupling”, *ChemArxiv* (2018)

[13] Stéphane Kéna-Cohen, and Joel Yuen-Zhou, “Polariton Chemistry: Action in the Dark”, ACS Central Science, (2019) Article ASAP

[14] T. W. Ebbesen, “Hybrid light–matter states in a molecular and material science perspective”, *Acc. Chem. Res*. 49, 2403– 2412 (2016).

[15] D. S. Dovzhenko, a S. V. Ryabchuk, a Yu. P. Rakovich a,b,c and I. R. Nabiev, “Light–matter interaction in the strong coupling regime: configurations, conditions, and applications”, *Nanoscale* 10, 3589 (2018)

[16] Manuel Hertzog, Mao Wang, Ju¨rgen Mony and Karl Borjesson, Strong light–matter interactions: a new direction within chemistry, DOI: 10.1039/c8cs00193f

[17] Mohammad H. Bitarafan and Ray G. DeCorby, “ On-Chip High-Finesse Fabry-Perot Microcavities for Optical Sensing and Quantum Information”, *Sensors* 17, 1748 (2017)

[18] A. Thomas, L. Lethuillier-Karl, K. Nagarajan, R. M. A. Vergauwe, J. George, T. Chervy, A. Shalabney, E. Devaux, C. Genet, J. Moran1, T. W. Ebbesen, "Tilting a ground-state reactivity landscape by vibrational strong coupling", *Science* 363, 615–619 (2019)

[19] Raphael F. Ribeiro, Luis A. Mart´ınez-Mart´ınez, Matthew Du, Jorge Campos-Gonzalez-Angulo and Joel Yuen-Zhou, "Polariton chemistry: controlling molecular dynamics with optical cavities", *Chem. Sci*. 9, 6325 (2018)

[20] T. E. Tessier, I. H. Deutsch, and A. Delgado, "Entanglement sharing in the two-atom Tavis-Cummings model", Physical Review A 68, 062316 (2003)

[21] M. Planck, *Verh. Dtsch. Phys. Ges*. 13, 138–148 (1911)

[22] A. Einstein and O. Stern, *Ann. Phys*., 345, 551–560 (1913)

[23] W. Nernst, Verh. Dtsch. Phys. Ges. 18, 83–116 (1916)

[24] E. Orgiu, J. George, J. Hutchison, E. Devaux, J. Dayen, B. Doudin, F. Stellacci, C. Genet, J. Schachenmayer and C. Genet, *Nat. Mater*., 2015, 14, 1123–1129

[25] Hutchison, J. A. et al. "Tuning the work-function via strong coupling" *Adv. Mater*. 25, 2481–2485 (2013).

[26] A. Vasanelli, Y. Todorov and C. Sirtori, *C. R. Phys*., 17, 861–873 (2016)

[27] Herrera, F.; Spano, F. C. Cavity-Controlled Chemistry in Molecular Ensembles. *Phys. Rev. Lett*. 116, 238301 (2016).

[28] Felipe Herrera, and Frank C. Spano, Theory of Nanoscale Organic Cavities: The Essential Role of Vibration-Photon Dressed States" *ACS Photonics* 5, 65-79 (2018)

[29] M. Ahsan Zeb, Peter G. Kirton, and Jonathan Keeling, "Exact States and Spectra of Vibrationally Dressed Polaritons" *ACS Photonics* 5, 249−257 (2018).

[30] S.J. Wang, A. Mika, J.A. Hutchison, C. Genet, A. Jouaiti, M.W. Hosseini, T.W. Ebbesen, "Phase transition of a perovskite strongly coupled to the vacuum field", *Nanoscale*, 6, 7243-7248 (2014)

[31]Principles of molecular photochemistry: An introduction, Nicholas J Turro, V. Raamurthy, J C Scaiano, *University Science Books*, *2015*

[32]Molecular spectroscopy, John M Brown, Oxford University press, New York, *2003*

[33]Specta of diatomic molecules, G Herzberg, van Nostrand, Princeton, NJ, *1950*

[34] Carl J. Seliskar and Richard E. Hoffmann, "Electronic spectroscopy of malondialdehyde", *Chem Phys Lett* 43, 2 (1976)

[35]The composition, structure and hydrogen bonding of diketones, John Emsley, Springer, Heidelberg, 1984.

[36]Vitaliy Feyer, Kevin C. Prince, Marcello Coreno, Sonia Melandri, Assimo Maris, Luca Evangelisti, Walther Caminati, Barbara M. Giuliano, Henrik G. Kjaergaard, and Vincenzo Carravetta, "Quantum Effects for a Proton in a Low-Barrier, Double-Well Potential: Core Level Photoemission Spectroscopy of Acetylacetone", *J. Phys. Chem. Lett*. 9, 521−526 (2018)

[37] R. Percy Barnes and Gladys Estelle Pinkney, Absorption Spectra of Some 1,3 Diketones, ACS (1953) **DOI:** 10.1021/ja01098a501

[38] W. F. Sager, N. Filipescu, and F. A. Serafín , “Substituent Effects on Intramolecular Energy Transfer. I. Absorption and Phosphorescence Spectra of Rare Earth ß-Diketone Chelates” *The Journal of Physical Chemistry*, 1964

[39] H. Henecka, “Chemie der Beta-Dicarbonyl-Verbindungen,” Springer Verlag, Berlin-Gottingen-Heidelberg, 1950.

[40] B. P. Kohler and R. P. Bernes, *ACS*, 66, 211 (1934).

[41] Felipe Antonio Pascal Hamilton, “Spectroscopy and Photochemistry of Aromatic and Cyclic Beta-Diketones” PhD dissertation, *Louisiana State University and Agricultural & Mechanical College,*1982.

[42] Kuo, J ., Ph.D. Dissertation, Louisiana State U n iversity, Baton Rouge, Louisiana (1966).

[43] Veierov, D ., Bercovici, T ., Fischer, E ., Mazur, Y. and Yogev, A ., J. Am. Chem. Soc., 8173 (1973).

[44]. Veierov, D ., Bercovici, T ., Fischer, E ., Mazur, Y. and Yogev, A ., *J. Am. Chem. Soc*., 99, 2723 (1977).

[45]. Markov, P ., Shishkova, L. and Radushev, A., *Tetrahedron*, 3203 (1973) 180

[46] Markov, P. and Petkov, I . , *Tetrahedron*, 33, 1013 (1977).

[47] Serge Haroche, A short history of Cavity Quantum Electrodynamics (2007) DOI: 10.1364/CQO.2007.CTuF2

[48] P. A. Hobson, W. L. Barnes, D. G. Lidzey, G. A. Gehring, D. M. Whittaker, M. S. Skolnick, and S. Walker, “Strong exciton–photon coupling in a low-Q all-metal mirror microcavity” *Appl. Phys. Lett.* 81, 3519 (2002)